Density Functional Theory Studies of Sulfur Compounds Removal by Zinc Oxide Nanotube

Sajjad Yari[1], Leila Mahdavian[1*], Negar Dehghanpour[2] and Dhameer A. Mutlak[3]

[1]*Department of Chemistry, Doroud Branch, Islamic Azad University, P.O. Box: 133. Doroud. Iran.*
[2]*Process Engineering Department, Lorestan Petrochemical Company, Bakhtar Petrochemical Holding, khoramabad, Iran.*
[3]*Materials and nuclear physics; Al-Nisour University College. Baghdad. Iraq.*

ABSTRACT

Selective adsorption of sulfur compounds is one of the most widely used methods. The most important advantages of this method are the desulfurization reaction at ambient temperature and pressure, which reduces the costs of refining operations. In this study, the reduction and elimination of sulfur pollutants (diethyl sulfide and benzothiophene) on zinc oxide nanotubes (ZnO-NT) has been investigated using DFT computational method. First, the geometric structures of the studied compounds were optimized and then the probabilities of approaching (passing through the central axis, adsorption on the top and wall of the nanotube) and adsorption and reduction of diethyl sulfide and benzothiophene to the oxidized nanotube were simulated in five steps. B3LYP/6-31++G* method was used to study the structural properties, thermodynamic parameters, and QSAR. The results showed that nanotubes show a high tendency to interact with both sulfur compounds in all spatial positions, so that the energy of the gap (E_g = 9.48 eV) decreases with the approach of the pollutant ($4 < E_g < 5$), which indicates the transfer of electrons between them. By studying the obtained structural properties and thermodynamic parameters, the tendency of ZnO-NT to adsorption of diethyl sulfide is higher than benzothiophene. While for both compounds, the position approaching the end of a ZnO-nanotube is more likely to pass through the central axis and adsorb on the outer wall of the nanotube. In general, this nano-adsorbent has the ability to adsorption of sulfur compounds and can reduce them, solving the problem of the oil industry.

Key words: Desulfurization, Sulfur compounds (diethyl sulfide and benzotiophenine), Zinc oxide nanotube (ZnO-NT), DFT-calculation

1. INTRODUCTION

In general, the amount of sulfur in crude oil varies from 0.03 to 7.89 wt% [1]. Sulfur compounds in crude oil include elemental sulfur, sulfide, disulfide, mercaptan, thiophene, and benzothiophene. Elimination of sulfur in crude oil is an important issue in the oil industry and related industries [2].

Complex sulfur compounds in crude oils increase their viscosity. Thio ethers and thiolans are easily removed by water and heat treatment during the desulfurization process. While sulfur in sulfurous aromatic compounds (such as benzothiophene, dibenzothiophene and benzoneftothiophene) are more resistant to remove by hydrodesulfurization and thermal conversion. Some important types of thiophenes are benzotiophenine and dibenzotiophenine which have one or two benzene groups

---

* Corresponding author: Leila.Mahdavian@iau.ac.ir

respectively. Elimination of sulfur in crude oil is an important issue in the oil and related industries [3]; they have toxic and corrosive effects on equipment [4].

There are various methods for separating sulfur compounds from oil reservoirs, including bio-desulfurization [5], adsorption desulfurization [6], extractive desulfurization [7], hydro-desulfurization [8], oxidative desulfurization, [9] and so on. The use of nano-sorbents by surface adsorption method is taken into consideration as one of the best methods, with low cost, simplicity, and high efficiency.

The identification and removal of diethyl sulfide and benzotiophenine pollutants in the environment are simulated and investigated by using zinc oxide nanotube (ZnO-NT (6-6)). In general, nanostructures due to their large surface-to-volume ratio (for example nanotubes, fullerenes, nano-clusters, and nano-cells) have many applications in areas such as adsorption [10, 11] transistors [12], catalysts [13], sensors [14], and medicine [15]. In new researches, the properties of materials can be increased by making changes in their structure. Recently, nanostructure which has two components $(XY)n$ (X and Y belong to the elements of groups III and V of the periodic table respectively) have been considered by many researchers [16-18]. Zinc oxide is a very important semiconductor material (due to its gap energy (3.37 eV) and bond energy) and it has a lot of applications such as nanosorbents, photocatalysts, optical sensors, solar cells, and highly emitting light emitting diodes (LEDs) [19-21]. As the dimensions of zinc oxide decrease to a smaller scale (nanometers), its properties change due to the effects of quantum size. Thus, the band gap energy is increased by quantum confinement [22]. The general purpose of this study is to investigate the thermodynamic, toxicity, and structural parameters of zinc oxide nanotube to remove sulfur compounds from petroleum compounds. The z-index files of their structure are simulated and optimized. Then, the interaction between pollutants and nano-sorbent is calculated and investigated with a method of B3LYP/6-31++G* by Wave-function Spartan series of programs [23, 24] The bond lengths, angles, active locations and sensitivity on the ZnO-NT structure (6-6) are investigated and the stages of pollutants approaching to the nano-adsorbent active sites are simulated and calculated. Figure 1 shows the structure of sulfur compounds. The diethyl sulfide, benzotiophenine, and ZnO-NT (6-6) are optimized by B3LYP/6-31++G* method. The sensitivity of ZnO-NT (6-6) is investigated by calculation of the HOMO, LUMO, and gap energy. If the energy gap (E_g) decreases with the pollutants closed to the ZnO-nanotube, it means that it generates an electrical signal and can detect these contaminants in the environment. Therefore, the NBO method is used to investigate the sensitivity of nanosorbents ZnO-NT (6-6).
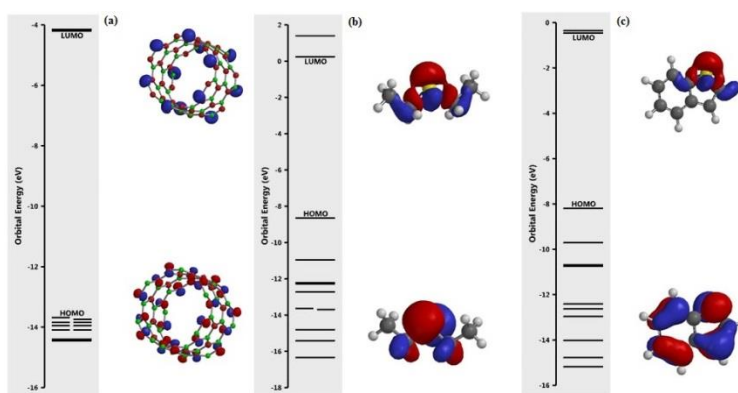

Figure 1. The ball and stick model of optimized geometrical structure: a) zinc oxide nanotube ZnO-NT (6-6), b) Diethyl sulfide ($C_4H_{10}S$) and c) Benzotiophenine (C_8H_6S) with HOMO and LUMO energy of them

One of the reasons for the spontaneous adsorption and reduction of pollutants by nanotubes in their various positions is the reduction of Gibbs free and enthalpy energy.

2. COMPUTATIONAL METHODS

Quantum chemistry has brought great changes in the science of chemistry by applying quantum mechanics. Theoretical study methods reduce the possibility of error and provide reliable confirmation for observations. To solve chemical problems, a series of molecular models or computational methods are used that predict the behavior of specific molecules in a chemical system. These computational methods are very much dependent on power as well as computer capabilities. Hence, with advances in computer science and programs related to computational methods, they have expanded very rapidly.

Zinc oxide nanoparticles are one of the most widely used mineral particles that have been considered by craftsmen due to their suitable physical and chemical properties. The special properties of zinc oxide nanoparticles are high chemical stability, low dielectric constant, high catalytic activity, infrared and ultraviolet light absorption, and most importantly antibacterial properties. The ZnO-NT (6-6) has a cylindrical structure that has been composed of a regular arrangement of zinc and oxygen atoms that is the same as the carbon arrangement in graphite plates [25, 26]. By arranging regular hexagons zinc and oxygen together, plates of their composition are formed. These plates are stacked on top of each other and each layer is connected to the bottom layer through weak van der Waals bonds. When these plates are intertwined, they form a zinc oxide nanotube. Now, the interaction between them is simulated according to the different positions of the pollutants in the presence of nanotube.

This study aims to investigate the thermodynamic, QSAR, and structural parameters and total energy of the mentioned interaction. Due to the interaction of the pollutant with the inner wall and the lack of recycling of the nanotube of ZnO (6-6), the interaction of the pollutant with the internal wall of a nanotube is not investigated. The two locations of the end (1st position) and the outer wall (2nd position) of the nanotube are considered for interaction with sulfur compounds (Figure 2). The QSAR computational method is used to investigate the compatibility of a nanotube with the environment that is a quantitative correlation between the structure and activity of chemical compounds.
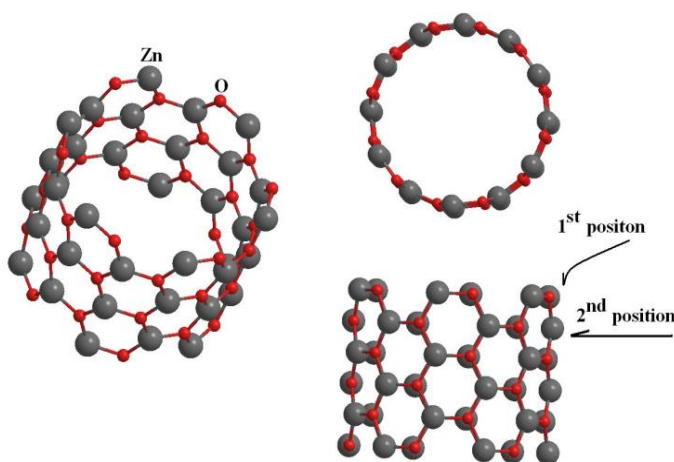
Figure 2. Optimized structure and different spatial positions of oxide nanotubes (ZnO-NT(6-6)) for passing and interacting with $C_4H_{10}S$ and C_8H_6S

3. RESULTS AND DISCUSSION

At first, the structure of ZnO-NT (6-6), diethyl sulfide, and benzotiophenine are separately optimized. Their thermodynamic, structural and environmental compatibility properties are calculated and evaluated. In this study, the structure of ZnO-NT (6-6) and pollutants are optimized and calculated of the thermodynamic properties, QSAR and structural parameters by B3LYP/6-31++G* method (Table 1). The results show that benzotiophenine is more stable than diethyl sulfide because its activation is less than di-ethyl sulfide and it contains higher entropy and lower enthalpy and Gibbs free energy. The zero-point energy is the smallest possible energy in a quantum mechanical system is lowest for benzotiophenine, indicating a high chemical activity of di-ethyl sulfide. In addition to studying the structure of pollutants, the thermodynamic parameters of ZnO-NT (6-6) with seat structure (6-6) with the number of atoms ($Zn_{36}O_{36}$) are given in Table 1.

Table 1. Thermodynamic properties of the pollutants and nano-adsorbent

	ZnO-NT(6-6)	$C_4H_{10}S$	C_8H_6S
E_{total}/a.u.	-2183.86	-48.06	492.26
Dipole moment/D	0.00	1.75	0.41
Symmetry group	S_4	C_{2V}	Cs
Zero point energy (ZPE)/kJ.mol^{-1}	793.79	341.44	299.76
H^o/a.u.	-0.47	0.119	0.309
G^o/a.u.	-0.62	0.08	0.27
C_v/J.mol^{-1}	602.80	79.43	92.23
S^o/J.mol^{-1}	1367.92	326.72	337.57

The relationship between chemical structure and biological activity is obtained by QSAR computational data. This computational model determines the effects of newly synthesized chemicals. In this study, a three-dimensional QSAR model was used to investigate the non-covalent interaction around bonded molecules, which can predict specificity through molecular descriptors and their coefficients. Table 2 shows the computational data of QSAR for investigating the environmental toxicity of this nano-sorbent. The obtained computational parameters (Min and Max Elpot/kJ.mol^{-1}) show that the environmental toxicity effect of benzotiophenine, which is an aromatic compound.

The stability and durability of benzothiophenine are higher than diethyl sulfide and its polarity parameter in the medium is more than the aliphatic form of the sulfur compound, so its dissolution rate is increased in polar solvents. Polarizability is the electronic distribution of a compound, the higher reactivity and is increased the effects of the compound in the environment. The data obtained for this parameter in Table 2 show confirmation of the previous results and further toxicity effects of benzothiophenine in the environment.

Table 2. QSAR calculations for the pollutants and the nano-adsorbent

Nano-Cage	ZnO-NT(6-6)	$C_4H_{10}S$	C_8H_6S
Area/Å^2	729.96	134.9	147.28
Volume/Å^3	589.17	107.53	133.89

PSA/Å^2	587.55	0.00	0.00
Ovality	2.33	1.23	1.16
Acc.Area/Å^2	575.59	125.46	143.21
P-Area(75)/Å^2	330.94	17.95	11.86
Acc.P-Area(75)/Å^2	270.05	12.8	11.86
Min Elpot/kJ.mol^{-1}	-144.53	-141.44	-101.89
Max Elpot/kJ.mol^{-1}	233.45	59.33	77.86
Min LocIonpot/kJ.mol^{-1}	60.09	49.26	60.43
Polarizability	39.14	48.0	50.41

To predict the type of products, their strength and stability in a chemical reaction are used from LUMO (the lowest unoccupied molecular orbit) and HOMO orbitals (the highest occupied molecular orbit). The interaction between molecules changes the energy level of HOMO and LUMO, which can affect the quantum properties of molecules such as electronegativity (η), chemical hardness (μ), chemical softness (σ), electrophilicity (ω), and molecular charge transfer (ΔN_{MAX}). The distance between the two energy levels of HOMO and LUMO is called the gap energy (E_g), which increases the structure of the compound to make it harder and less reactive. The quantum properties of molecules can be calculated from the following relationships [25- 28]:

$$E_g = E_{LUMO} - E_{HOMO} \tag{1}$$
$$\eta = (E_{LUMO} + E_{HOMO})/2 \tag{2}$$
$$\mu = (E_{LUMO} - E_{HOMO})/2 \tag{3}$$
$$\sigma = 1 - \mu \tag{4}$$
$$\omega = \eta^2/2\,\mu \tag{5}$$
$$\Delta N_{MAX} = -\eta/\mu \tag{6}$$

Table 3 shows all the quantum parameters obtained by the above equations for nanotube and pollutants. According to Eq. (7), the relationship between electrical conductivity (E_c) and gap energy (E_g) can be obtained from:

$$E_c \propto \exp(-E_g/2KT) \tag{7}$$

where K is the Boltzmann constant and T is the ambient temperature. Eq. (7) shows that reducing the amount of gap energy (E_g) causes increase conductivity and electrical conductivity of the compound or complex, so the results show benzothiophene has a softer structure and more conductivity than the aliphatic compound of diethyl sulfide.

Table 3. Electrical structure parameters of the nanotube and pollutants

	E_{LUMO}/eV	E_{HOMO}/eV	E_g/eV	η/eV	μ/eV	σ/eV	ω/eV	ΔN_{MAX}/eV
ZnO-NT(6-6)	-4.20	-13.68	9.48	-8.94	4.74	-3.74	8.43	1.89
C$_4$H$_{10}$S	0.24	-8.66	8.9	-4.21	4.45	-3.45	1.99	0.946
C$_8$H$_6$S	-0.46	-8.20	7.74	-4.33	3.87	-2.87	2.42	1.12

The smaller the LUMO-HOMO strip gap, the softer the structure and the better the electron transfer process. Thus, the molecular charge-transfer (ΔN_{MAX}) reflects the electron donor or receivability of

the pollutants and the nano adsorbent. The ΔN_{MAX} positive means the transfer of electrons in chemical reactions from the nano adsorbent to the pollutant.

After simulating and optimizing the structures of ZnO-NT (6-6), diethyl sulfide, and benzothiophene, all probabilities and active sites of pollutants interaction with ZnO-NT (6-6) are investigated. Figure 3 shows all the active sites and probabilities of pollutants approaching the ZnO-NT (6-6). Due to the structure of the selected nanotube, all the atoms at the end of the nanotube have the same position in comparison with each other and all the atoms in the wall of it have the same position.
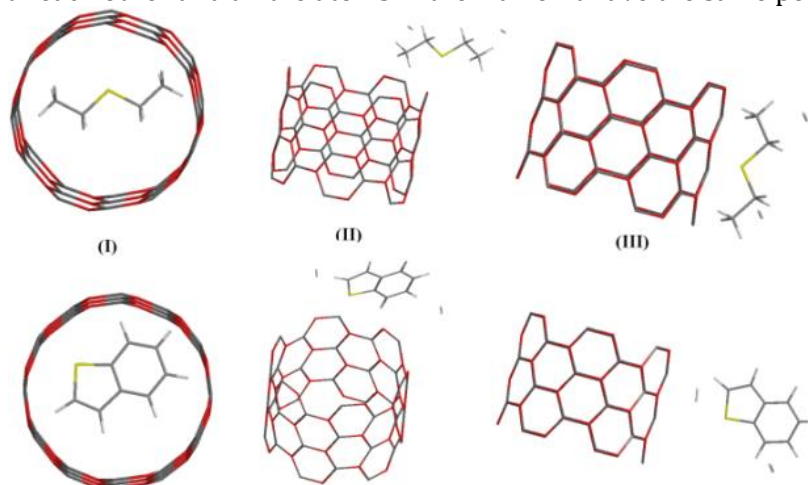

Figure 3. Approaching the pollutants to ZnO-NT(6-6) at different spatial positions, I) central axis, II) end and III) wall of ZnO-NT(6-6)

There are three spatial positions for the proximity of the pollutants to a nanotube. In spatial positions 1 and 2 (Figure 3), due to the exchange of electrons between them, the following chemical interaction occurs and causes the removal of the H_2S molecule from the pollutants, and the reaction for C_8H_6S is as follows:

ZnO-NT + C_8H_6S + $2H_2$ → ZnO-NT....C_8H_6S + $2H_2$ (1st, 2nd and 3rd steps)
ZnO-NT....C_8H_6S + $2H_2$ → C_8H_8 + ZnO-NT.... H_2S (4th step)
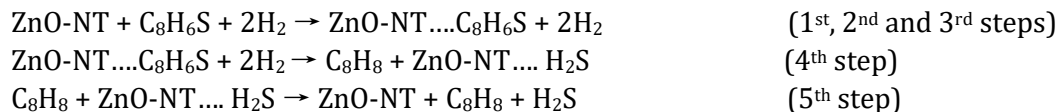C_8H_8 + ZnO-NT.... H_2S → ZnO-NT + C_8H_8 + H_2S (5th step)

Figure 4 shows the steps of approaching the benzothiophenine to the end position on zinc oxide-NT.
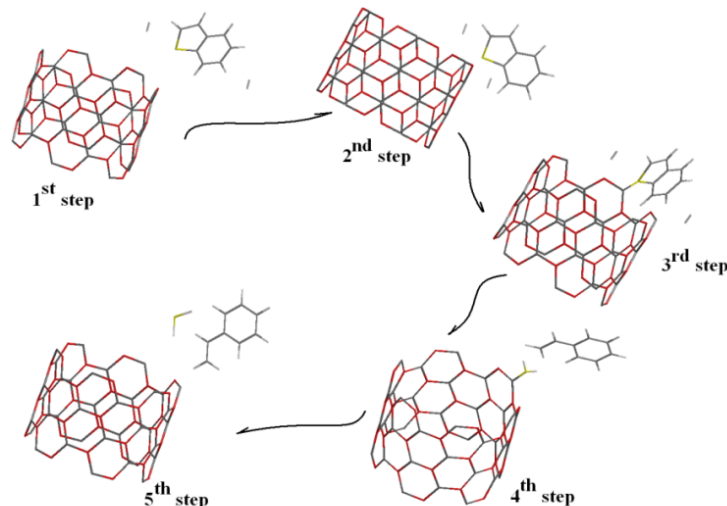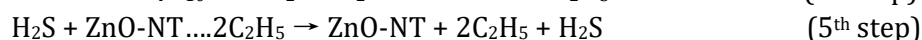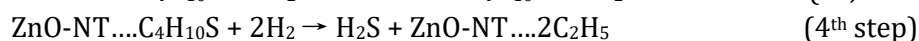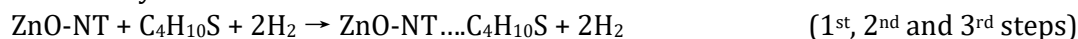
Figure 4. Stick model of benzothiophenine (C_8H_6S) interaction with the ZnO nanotube in the first position

For diethyl sulfide:

$ZnO-NT + C_4H_{10}S + 2H_2 \rightarrow ZnO-NT....C_4H_{10}S + 2H_2$ (1st, 2nd and 3rd steps)

$ZnO-NT....C_4H_{10}S + 2H_2 \rightarrow H_2S + ZnO-NT....2C_2H_5$ (4th step)

$H_2S + ZnO-NT....2C_2H_5 \rightarrow ZnO-NT + 2C_2H_5 + H_2S$ (5th step)

3.1 Thermodynamic Properties

The thermodynamic parameters of the interaction of diethyl sulfide and benzotiophenine with nanotube are shown in Tables 4 to 6. In the passing of pollutants through the central axis of the nanotube, the dipole moment of diethyl sulfide increases with approaching to nanotube in 1st and 2nd step. In the 2nd steps, the enthalpy and Gibbs free energy are less, and the 5th step has more entropy, in which case the calculated dipole moment is less as well. For benzothiophenine pollutants, the first stage has less enthalpy and Gibbs free energy. In terms of entropy, the 3rd step also has more irregularity, in which case the calculated dipole moment is also lower. Diethyl sulfide shows a greater tendency to pass from the central axis of the ZnO nanotube, which can be related to its stability and structural symmetry. The results of the passing of the pollutant through the central axis of the nanotube show that initially the nanotube shows a high tendency to pull inside both pollutants, but in the middle of the tube it repels it due to the force field entered by the nanotube.

Table 4. Thermodynamic properties of the diethyl sulfide and benzothiophenine passing from a central axis of ZnO-NT

ZnO-Nanotube	Diethyl sulfide					Benzothiophenine				
	1	2	3	4	5	1	2	3	4	5
E_{total}/a.u.	-2259.01	-2263.92	-2411.04	-2744.30	-2724.99	-1995.84	-1990.82	-509.58	-814.64	-1754.17
Dipole moment/D	2.61	3.61	1.77	1.75	1.06	2.50	3.32	1.15	0.86	1.89
Zero point energy	1136.59	1131.13	1137.97	1173.07	1129.63	1091.34	1090.60	1095.33	1097.75	1103.47

(ZPE)/kJ.mol⁻¹										
Hº/a.u.	-0.36	-0.36	0.34	0.23	-0.16	-0.28	-0.27	0.29	0.17	-0.18
Gº/a.u.	-0.53	-0.53	0.18	0.06	-0.33	-0.44	-0.44	0.12	0.007	-0.35
C_v/J.mol⁻¹	682.09	683.05	685.01	677.48	685.77	699.36	700.10	703.92	700.02	700.00
Sº/J.mol⁻¹	1485.20	1492.45	1487.04	1469.07	1494.43	1483.16	1482.63	1498.59	1483.68	1482.54

The zinc oxide nanotube tends to absorb sulfur compounds. According to the calculated structural parameters for the nano-sorbent, the two positions of the wall and end of the nanotube are the chemically active site for the adsorption of pollutants (Fig.2). Table 5 shows the thermodynamic parameters of the conversion of diethyl sulfide and benzothiophenine on the end of ZnO-nanotube.

In the 3rd step, an interface is created between the pollutant and the nanotube. In the 4th step, the electron exchange of the product occurs, which is the release of H_2S gas which the bipolar moment reaches its maximum amount at this stage and indicates the progress of the reaction to the products. That it is the removal of sulfur atoms from the composition. Other thermodynamic parameters indicate the spontaneity of the reaction and the tendency of the nanotube to exchange electron and the reaction to remove H_2S gas.

Adsorption of benzothiophenine pollutant on the end of nanotube, 2nd and 3rd steps have less enthalpy and Gibbs free energy. The obtained entropy values also confirm this, the reactions always lead to more irregularities. The calculated bipolar moment is also less.

Table 5. Thermodynamic properties of the diethyl sulfide and benzothiophenine adsorption and converted to products on end of ZnO-NT

ZnO-Nanotube	Diethyl sulfide					Benzothiophenine				
	1	**2**	**3**	**4**	**5**	**1**	**2**	**3**	**4**	**5**
E_{total}/a.u.	-2267.5	-2037.4	-1789.08	-2447.00	-2495.45	-1855.5	-1781.6	-998.87	-1615	-1772.36
Dipole moment/D	1.49	1.99	5.74	11.57	9.47	0.62	0.95	4.53	3.40	7.75
Zero point energy (ZPE)/kJ.mol⁻¹	1215.30	1215.1	1222.69	1236.8	1218.37	1152.84	1152.3	1154.91	1141.8	1152.66
Hº/a.u.	-0.33	-0.24	-0.14	-0.52	-0.41	-0.20	-0.17	-0.20	-0.11	-0.16
Gº/a.u.	-0.50	-0.41	-0.32	-0.35	-0.59	-0.37	-0.34	-0.38	-0.28	-0.33
C_v/J.mol⁻¹	711.48	713.43	709.17	699.04	707.25	729.42	728.01	727.01	730.82	727.12
Sº/J.mol⁻¹	1533.57	1539.1	1533.36	1508.8	1525.90	1537.30	1529.6	1527.15	1537.8	1527.20

Computational data of the adsorption and conversion of both pollutants on the wall of zinc oxide nanotubes are shown in Table 6. From the results, the end of the nanotube shows a greater tendency to adsorb and convert pollutants. They show that the wall spatial position of the nanotube tends to adsorb and convert diethyl sulfide.

The rate of structural change and electron transfer is greater as pollutants approach to the end of the nanotube. The adsorption reaction is most stable, has the most negative energy, enthalpy (ΔH), and free energy (ΔG), and also has the highest entropy (ΔS).

Comparing the data obtained in Tables 4 to 6, both contaminants are more likely to interact with the end of nanotube. The electron transfer between the nanotube and the pollutant has occurred. This interaction is beneficial to the system and brings more stability. In comparison with the two pollutants, the lowest energy is related to diethyl sulfide, which has a high electron density. In all structures, the contaminant moves along the length after conversion and moves away from the edges. It can be concluded that the interactions that were closer to the active sites of the nanotube were more favorable for the system.

Table 6. Thermodynamic properties of the diethyl sulfide and benzothiophenine adsorption and converted to products on the wall of ZnO-NT

ZnO-Nanotube	Diethyl sulfide					Benzothiophenine				
	1	**2**	**3**	**4**	**5**	**1**	**2**	**3**	**4**	**5**
E_{total}/a.u.	-2273.98	-1844.4	-1503.66	-1627.5	-1917.1	-1855.37	-1875.2	-813.92	-2666.3	-2672.58
Dipole moment/D	1.56	2.09	10.46	6.28	6.80	0.54	1.92	7.32	8.80	9.05
Zero point energy (ZPE)/kJ.mol^{-1}	1206.53	1214.40	1244.94	1227.9	1222.4	1152.89	1153.59	1194.24	1175.5	1151.08
H^o/a.u.	-0.33	-0.17	1.12	-0.08	-0.19	-0.19	-0.20	0.21	1.53	0.48
G^o/a.u.	-0.51	-0.34	0.94	-0.25	-0.37	-0.37	-0.38	0.04	1.36	0.30
C_v/J.mol^{-1}	716.25	715.12	715.39	704.59	706.13	729.39	729.48	721.88	720.43	728.04
S^o/J.mol^{-1}	1540.87	1546.23	1534.98	1512.8	1519.9	1537.34	1529.91	1512.14	1508.1	1528.41

3.2 The Electron Structure Parameters

Tables 7 and 8 show the structural parameters computed for the interactions. For ions and polyatomic molecules, hardness and softness are closely related to HOMO and LUMO energy. With the formation of the complex (steps), the gap energy (E_g) increases so the structure becomes harder. This means that the chemical species are softer, the gap energies are smaller, and are more reactivity occurs between them. The E_g is calculated for ZnO-NT (6-6) (E_g= 9.489 eV), both pollutants are reduced by closing it. For adsorption of diethyl sulfide on the end of ZnO-NT, this reduction reaches 4.53 eV, indicating a greater tendency of the end of the nanotube to react with sulfur compounds (Table 7).

The HOMO and LUMO energy level have changed for steps 1 to 5. The gap energy (E_g) increases with the entry of sulfur compounds into the nanotube up to the fourth stage, which indicates a decrease in the conductivity of the nanotube by passing these compounds through the central axis, and conductivity has increased in 5th step (Tables 7 and 8).

Table 7. Electrical structure parameters of the interaction of diethyl sulfide and nanotubes

Nano-Sorbent	State	E_{LUMO}/eV	E_{HOMO}/eV	E_g/eV	η /eV	μ /eV	σ/eV	ω/eV	ΔN_{MAX}/eV
Passing of Diethyl sulfide in central axis of nanotube	ZnO-NT(6-6)	-4.20	-13.68	9.48	-8.94	4.74	-3.74	8.43	1.89
	1	-4.13	-9.26	5.13	-6.69	2.56	-1.56	8.74	2.61
	2	-4.10	-9.89	5.79	-6.99	2.89	-1.89	8.45	2.42
	3	-4.32	-10.24	5.92	-7.28	2.96	-1.96	8.95	2.46
	4	-4.28	-10.37	6.09	-7.32	3.04	-2.04	8.81	2.40
	5	-4.24	-9.89	5.65	-7.06	2.82	-1.82	8.84	2.50
Adsorption of Diethyl sulfide on end of nanotube	1	-4.18	-8.71	4.53	-6.44	2.26	-1.26	9.17	2.85
	2	-4.15	-8.99	4.84	-6.57	2.42	-1.42	8.91	2.71
	3	-4.15	-9.58	5.43	-6.86	2.71	-1.71	8.68	2.53
	4	-4.02	-12.24	8.22	-8.13	4.11	-3.11	8.04	1.98
	5	-4.01	-11.98	7.97	-7.99	3.98	-2.98	8.02	2.00
Adsorption of Diethyl sulfide on outer wall of nanotube	1	-4.18	-8.78	4.60	-6.48	2.30	-1.30	9.13	2.82
	2	-4.16	-9.14	4.98	-6.65	2.49	-1.49	8.88	2.67
	3	-4.07	-9.79	5.72	-6.93	2.86	-1.86	8.40	2.42
	4	-3.95	-10.92	6.97	-7.43	3.48	-2.48	7.93	2.13
	5	-3.99	-11.49	7.50	-7.74	3.75	-2.75	7.99	2.06

Molecular orbital analysis (HOMO - LUMO) shows that the molecular orbitals of HOMO for the two pollutants in all states are on the surface of pollutants-zinc oxide nanotube. The molecular orbitals of LUMO are just on the nanotubes. The obtained data show that the electron transfer between benzothiophenine is higher than diethyl sulfide because is related to its aromatic structure.

In their structures, ΔN_{MAX}/eV shows that the distribution of electron charge is continuous between the pollutant and nanotube, and indicates the presence of chemical interaction and electron transfer between them. In general, increasing the softness, decreasing the hardness and gap energy with the pollutants approaching the nanotube indicates a higher reactivity and different locations of the nanotube, thus having a more suitable loading property to reduce sulfur compounds.

Table 8. Electrical structure parameters of benzothiophenine and ZnO-NT nanotube

Nano- Sorbent	State	E_{LUMO}/eV	E_{HOMO}/eV	E_g/eV	η /eV	μ /eV	σ/eV	ω/eV	ΔN_{MAX}/eV
Passing of benzothiophenine in central axis of nanotube	ZnO-NT(6-6)	-4.20	-13.68	9.48	-8.94	4.74	-3.74	8.43	1.89
	1	-4.14	-9.19	5.05	-6.66	2.52	-1.52	8.80	2.64
	2	-4.16	-9.89	5.73	-7.02	2.86	-1.86	8.61	2.45
	3	-4.28	-10.46	6.18	-7.37	3.09	-2.09	8.79	2.38
	4	-4.24	-10.29	6.05	-7.26	3.02	-2.02	8.73	2.40
	5	-4.20	-10.31	6.11	-7.25	3.05	-2.05	8.62	2.37
Adsorption of benzothiophenine on end of nanotube	1	-4.19	-8.68	4.49	-6.43	2.24	-1.24	9.22	2.87
	2	-4.14	-8.95	4.81	-6.54	2.40	-1.40	8.91	2.72
	3	-4.04	-9.77	5.73	-6.90	2.86	-1.86	8.32	2.41

	4	-3.96	-9.82	5.86	-6.89	2.93	-1.93	8.10	2.35
	5	-3.95	-9.97	6.02	-6.96	3.01	-2.01	8.05	2.31
Adsorption of benzothiophenine on outer wall of nanotube	**1**	-4.19	-8.75	4.56	-6.47	2.28	-1.28	9.18	2.84
	2	-4.17	-9.07	4.90	-6.62	2.45	-1.45	8.94	2.70
	3	-4.09	-9.54	5.45	-6.81	2.72	-1.72	8.52	2.50
	4	-4.12	-9.35	5.23	-6.73	2.61	-1.61	8.67	2.58
	5	-4.03	-9.67	5.64	-6.85	2.82	-1.82	8.32	2.43

The adsorption energy (E_{ad}) of the interaction between them is calculated by the following equation:

$$E_{ad}=E_{X-NT} - [E_X+E_{NT}] \tag{8}$$

In this equation, the E_{x-NT}, E_x, and E_{NT} are the total energy of the created complex in the adsorption of pollutant on the ZnO-nanotube, the total energy of the pollutant, and the nanotube energy respectively.

Table 9 shows the sulfur compounds on nanoorbentss indicating the chemical adsorption. The interaction of chemicals between them increases the adsorption energy. This energy is much higher than the adsorption energies in the physical adsorption range, so this adsorption is considered chemical. The structure of sulfur compounds after adsorption in different places of nanotubes undergoes significant changes. The exchange of electrons between them releases sulfur atoms in the form of H_2S.

Table 9. Adsorption energy (E_{ad}/eV) of the diethyl sulfide and benzothiophenine passing, adsorption and converted to products by ZnO-NT

ZnO-Nanotube	Diethyl sulfide			Benzothiophenine		
	Passing	Adsorption on end	Adsorption on wall	Passing	Adsorption on end	Adsorption on wall
1	-27.09	-35.58	-42.06	-304.24	-163.90	-163.77
2	-32.00	194.52	387.52	-299.22	-90.00	-183.60
3	-179.12	442.84	48.06	1182.02	692.73	877.68
4	-512.38	-215.08	604.42	876.96	76.6	-974.70
5	-493.07	-263.53	314.82	-62.57	-80.76	-980.98

4. CONCLUSION

In this study, the efficiency and sensitivity of zinc oxide nanotubes is investigated in terms of thermodynamics and electricity against sulfur contaminants such as diethyl sulfide and benzothiophene by B3LYP/6-31++G* method. Using the NBO method, the amount of HOMO and LUMO energy is calculated. The probability of the contaminants interacting with the zinc oxide nanotubes is simulated and the proposed mechanism is investigated thermodynamically and structurally. Three probabilities of pollutants passing through the central axis, their adsorption, and conversion were evaluated on the end and wall of the nanotube.

Reducing the amount of free energy and enthalpy of reaction formation indicates that the proposed probabilities are desirable and spontaneous. Increasing the entropy of different positions of nanotubes against pollutants indicates the greater probability of that state in the real environment. The results show that the spatial positions of ZnO nanotubes act the same for two pollutants. For both pollutants, they are more likely to be adsorbed on top of the nanotube than on the wall. Interaction of aliphatic compounds with zinc oxide nanotubes is also more likely. As the sulfur compounds approach, the conductivity of the oxide nanotube increases. Computational data show that oxidized nanotubes work well to identify and desulfurize aliphatic and aromatic compounds and can be used in sensors, filters, and nanosorbents.

Authors' Contribution:
Study concept and design: Sajjad Yari, Leila Mahdavian, Negar Dehghanpour and Dhameer A. Mutlaki.
Analysis and in terpretation of data: Leila mahdavian and Dhameer A. Mutlaki.
Drafting of the manuscript: Sajjad Yari, Leila Mahdavian and Negar Dehghanpour.
Critical revision of the manuscript for important intellectual content: Sajjad Yari, Leila Mahdavian, Negar Dehghanpour and Dhameer A. Mutlaki.
Statistical analysis: Sajjad Yari, Leila Mahdavian and Dhameer A. Mutlaki.
Administrative, technical, or material support: Sajjad Yari, Leila Mahdavian, Negar Dehghanpour and Dhameer A. Mutlaki and Supervision: Leila Mahdavian and Dhameer A. Mutlaki.

References:

[1] Y. Zhigang, M. Xuguang, S. Jiuhua, Y. Xiaorong, T. Qiong. Investigations in enhancement biodesulfurization of model compounds by ultrasound pre-oxidation. Ultrasonics Sonochemistry. 54, 2019, 110-120.

[2] D.F. Silva, A.M. Viana, F. Mirante, B. de Castro, L.C. Silva, S.S. Balula. Removing Simultaneously Sulfur and Nitrogen from Fuel under a Sustainable Oxidative Catalytic System. Sustain. Chem. 2, 2021, 382–391.

[3] W. Tang, J. Gu, H. Huang, D. Liu, C. Zhong. Metal‐organic frameworks for highly efficient adsorption of dibenzothiophene from liquid fuels. J. AIChE, 62(12), 2016, 4491-4496.

[4] R. Ullah, P. Bai, P. Wu, B. Liu, F. Subhan, Z.Yan. Cation–anion double hydrolysis derived mesoporous mixed oxides for reactive adsorption desulfurization. J. Microporous Mesoporous Mater. 238, 2017, 36–45.

[5] D. Juliao, F. Mirante, S.O. Ribeiro, A.C. Gomes, R.Valenca, J.C. Ribeiro, M. Pillinger, B. de Castro, I.S. Goncalves, S.S. Balula. Deep oxidative desulfurization of diesel fuels using homogeneous and SBA-15-supported peroxophosphotungstate catalysts. Fuel. 241, 2019, 616–624.

[6] H.H. El-Maghrabi, R.S. Mohamed, A.A. Younes. Reduction of sulfur oxides emissions via adsorptive desulfurization of transportation fuels using novel silica-based adsorbent. Environ Sci Pollut Res. 2021. https://doi.org/10.1007/s11356-021-14039-6.

[7] E. Syntyhaki, D. Karonis. Oxidative and extractive desulfurization of petroleum middle distillates, using imidazole ionic liquids. Fuel Communications. 7, 2021, 100011.

[8] L. Zhang, X. Chen, C. Liang. Improving the hydrodesulfurization performance of the sulfur-resistant intermetallic Ni_2Si based on a MOF-derived route. Inorganic Chemistry Frontiers. 8, 2021, 1122-1127.

[9] X.B. Lim, W.J. Ong. A current overview of the oxidative desulfurization of fuels utilizing heat and solar light: from materials design to catalysis for clean energy. anoscale Horiz. 2021. https://doi.org/10.1039/D1NH00127B.

[10] A. S. Rad, S. S. Shabestari, S. Mohseni, S. A. Aghouzi. Study on the adsorption properties of O_3, SO_2, and SO_3 on B-doped graphene using DFT calculations. Journal of Solid State Chemistry. 237, 2016, 204-210.

[11] R. Jeswani, Y. Patil, S. Patil. Intravenous magnesium sulfate and isoxsuprine for arrest of preterm labor: A comparative study. Journal of Natural Science, Biology and Medicine, 12(2), 2021, 135-135.

[12] D.A. Wild, T. Lenzer. Structures and infrared spectra of fluoride-hydrogen sulfide clusters from ab initio calculations: F(-)-(H2S)n, n = 1-5. Phys. Chem. Chem. Phys. 7(22), 2005, 3793-804.

[13] S. Sarkar, M. Monu, B. Bandyopadhyay. Cooperative nature of the sulfur centered hydrogen bond: investigation of $(H_2S)n$ (n = 2–4) clusters using an affordable yet accurate level of theory. Physical Chemistry Chemical Physics. 49, 2019, 10-21.

[14] M. Salimi, V. Pirouzfar, E. Kianfar. Enhanced gas transport properties in silica nanoparticle filler-polystyrene nanocomposite membranes. Colloid Polym Sci 295, 2017, 215–226.

[15] S. Ghotekar, T. Pagar, S. Pansambal, R. Oza. A Review on Green Synthesis of Sulfur Nanoparticles via Plant Extract, Characterization and its Applications. Adv. J. Chem. B. 2(3), 2020, 128-143.

[16] I.V. Boyko, M.R. Petryk. Interaction of electrons with acoustic phonons in AlN/GaN resonant tunnelling nanostructures at different temperatures. Condens. Matter Phys. 23(3), 2020, 33708.

[17] O. Mikhailov, D. Chachkov, Novel oxdationdegree-Zn+3 in the macrocyclic compound with trans-DI [BENZO] prophyrazine and fluoride ligand: quantum-chemical consideration. European Chemical Bulletin, 9(7), 2020,160-163.

[18] M. Rakebizadeh, M. Zahedizadeh, Y. E. Panah. Supplemental Effect of Zinc Oxide Nanoparticles and Mentha spicata butanol Extract on Blood Glucose of Diabetic Wistar Rats. Journal of Research in Science, Engineering and Technology, 6(03), 2018, 1-5.

[19] W, Abdussalam-Mohammed. Comparison of Chemical and Biological Properties of Metal Nanoparticles (Au, Ag), with Metal Oxide Nanoparticles (ZnO-NPs) and their Applications. Adv. J. Chem. A. 3(2), 2020, 192-210.

[20] T. Poojary, K. Sudha, K. Sowndarya, R. Kumarachandra, Y. Durgarao. Biochemical role of zinc in dengue fever. Journal of Natural Science, Biology and Medicine, 12(2), 2021, 131-131.

[21] R. A. A. Madlol. Structural and optical properties of ZnO nanotube synthesis via novelmethod.Results in Physics. 7, 2017, 1498–1503.

[22] Z. Fan, J. Lu. Zinc oxide nanostructures: synthesis and properties. J Nanosci Nanotechnol. 5, 2005, 1561-1573.

[23] Wavefunction Spartan 14 v1.1.4**.**

[24] O. V. Mikhailov, D. V. Chachkov, Molecular structure models of Al_2Ti_3 and Al_2V_3 clusters according to DFT quantum-chemical calculations. European Chemical Bulletin, 9(2), 2020, 62-68.

[25] A. Ali, A.R. Phull, M. Zia. lemental zinc to zinc nanoparticles: is ZnO NPs crucial for life, Synthesis, toxicological, and environmental concerns. Nanotechnology Reviews. 7(5), 2018, 413-441.

[26] Gözükızıl, M. F. pH effect on structural, morphological and optical properties of ZnO thin films produced by chemical bath deposition method. European Chemical Bulletin, 9(10), 2020, 335-338.

[27] M.E. Belghiti, S. Echihi, A. Mahsoune, Y. Karzazi, A. Aboulmouhajir, A. Dafali, I. Bahadur. Piperine derivatives as green corrosion inhibitors on iron surface; DFT, Monte Carlo dynamics study and complexation modes. J. Mol. Liq. 261, 2018, 62-75.

[28] P. G. Pathare, S. U. Tekale, M. G. Damale, J. N. Sangshetti, R. U. Shaikh, L. Kótai, , R. P. P. Silaev. Pyridine and benzoisothiazole based pyrazolines: synthesis, characterization, biological activity, molecular docking and admet study. European Chemical Bulletin, 9(1), 2020, 10-21.